# INTEGRATION OF GEOMATICS METHODOLOGIES AND CREATION OF A CULTURAL HERITAGE APP USING AUGMENTED REALITY

*INTEGRACIÓN DE METODOLOGÍAS GEOMÁTICAS Y CREACIÓN DE UNA APLICACIÓN PATRIMONIAL USANDO REALIDAD AUMENTADA*

Vincenzo Barrile[a] , Antonino Fotia[a] , Giuliana Bilotta[a,b,*] , Domenico De Carlo[a]

[a] Department of Civil, Energy, Environment and Materials Engineering (DICEAM), University Mediterranea of Reggio Calabria, via Graziella, Feo di Vito, 89128 Reggio Calabria, Italy. vincenzo.barrile@unirc.it; antonino.fotia@unirc.it; domenico.decarlo@unirc.it

[b] Department of Planning, University IUAV of Venice, Santa Croce 191 Tolentini, 30135 Venice, Italy. giuliana.bilotta@iuav.it

**Highlights:**

- Use of different algorithms for registration of terrestrial laser scans and analysis of the data obtained.
- 3D acquisition, processing and restitution methodology from georadar data.
- Implementation of a tourist app in both virtual and augmented reality by integrating geomatics methodologies.

**Abstract:**

3D modelling of archaeological and historical structures is the new frontier in the field of conservation science. Similarly, the identification of buried finds, which enhances their multimedia diffusion and restoration, has gained relevance. As such sites often have a high level of structural complexity and complicated territorial geometries, accuracy in the creation of 3D models and the use of sophisticated algorithms for georadar data analysis are crucial. This research is the first step in a larger project aimed at reclaiming the ancient villages located in the Greek area of southern Italy. The present study focuses on the restoration of the village of Africo (RC), a village hit by past flooding. The survey began with a laser scan of the church of St. Nicholas, using both the Faro Focus3D and the Riegl LMS-Z420i laser scanner. At the same time, georadar analyses were carried out in order to pinpoint any buried objects. In the processing phase, our own MATLAB algorithms were used for both laser scanner and georadar datasets and the results compared with those obtained from the scanners' respective proprietary software. We are working to develop a tourism app in both augmented and virtual reality environments, in order to disseminate and improve access to cultural heritage. The app allows users to see the 3D model and simultaneously access information on the site integrated from a variety of repositories. The aim is to create an immersive visit, in this case, to the church of St. Nicholas.

**Keywords:** laser scanner; 3D modelling; ground penetrating radar (GPR); archaeological and historical structures; augmented reality (AR)

**Resumen:**

El modelado 3D de estructuras arqueológicas e históricas es el nuevo hito en el campo de la ciencia de la conservación. De manera similar, la identificación de hallazgos enterrados ha ganado relevancia, ya que mejora la difusión multimedia y la restauración. Como a menudo los sitios en estudio tienen un alto nivel de complejidad estructural y geometrías territoriales complicadas, la precisión en la creación de modelos 3D y el uso de algoritmos sofisticados para el análisis de datos georradar son puntos cruciales. Esta investigación es el primer paso en un proyecto más grande destinado a recuperar las aldeas antiguas de la zona griega al sur de Calabria. El presente estudio se centra en la restauración de la aldea Africo (RC), que fue golpeada en el pasado por una inundación. El trabajo comenzó con el análisis de los datos láser de la iglesia de San Nicolás en el centro del pueblo, utilizando el láser escáner Faro Focus3D y el Riegl LMS-Z420i. Paralelamente, se llevaron a cabo análisis georradar para resaltar cualquier objeto enterrado. En la fase de procesamiento, se utilizaron nuestros algoritmos desarrollados en MATLAB para ambos conjuntos de datos, escáner láser y georradar. Los resultados se compararon con los obtenidos con el software propietario respectivo. Estamos trabajando en el desarrollo de una aplicación turística en entornos de realidad virtual y aumentada que permita difundir y apreciar el patrimonio cultural. Por consiguiente, la aplicación mencionada se ha implementado de manera que permita al usuario ver el modelo 3D y la información en realidad aumentada. Con la realidad aumentada, de hecho, intentamos que haya más información disponible de otros repositorios integrándolos con monumentos, bellezas naturales, rincones característicos, creando así las condiciones para una visita inmersiva, en el caso aquí propuesto la iglesia de San Nicolás.

**Palabras clave:** láser escáner; modelado 3D; georradar (GPR); estructuras arqueológicas e históricas; realidad aumentada (RA)

---

*Corresponding author: Giuliana Bilotta, giuliana.bilotta@iuav.it

## 1. Introduction

The village of Africo Vecchio is located in the heart of the Aspromonte National Park at an altitude of about 700 m above sea level. The village was founded in the 9th century AD, but was abandoned after the great flooding of 1951 which subsequently moved further along the Ionian coast, and was renamed as Africo. The Byzantine church of S. Leo is situated close to Africo Vecchio; behind it, supposedly, are the ruins of an ancient monastery and/or ancient underground cisterns for water collection. Investigations with laser scanners and ground penetrating radar (GPR) aim to rebuild the ground morphology by recreating the three dimensional (3D) model and identifying areas that may be subject to future archaeological excavations.

The Apennine Mountains located in the southern Italian region of Calabria, witnessed a remarkable development in monasticism by Basilica monks during the 5th and 12th centuries. Over that period, they built a series of monasteries and churches that represent a cultural heritage of great historical and artistic value. Investigations conducted with GPR and terrestrial laser Scanning (TLS) behind the church of S. Leo (Africo Vecchio, RC, see Figure 1) were performed according to the instructions of academics. Laser scanner and georadar were adopted as non-invasive instruments during the data acquisition phase. The data processing phase was carried out with both our own MATLAB algorithms and commercial software in order to validate the results obtained.



**Figure 1**: View of the Church of Africo Vecchio.

## 2. Materials and Methods

### 2.1. Terrestrial laser scanning

The laser scanner proved to be a very important tool in this cultural context. Due to its non-invasiveness, it allows a greater degree of inspection without damaging the historical artistic and economic value of the site.

The aim of the survey is to reconstruct a 3D model of the church in question by comparing two different data acquisition and processing methods with two different laser scanners in order to evaluate their accuracy (Ballabeni, Apollonio, Gaiani, & Remondino, 2015).

The following procedures were followed:

- 3D pad with Riegl LMS-Z420i laser scanner;
- Data processing through the Iterative Closest Point (ICP) algorithm;
- A 3D survey with FARO HE80 laser scanner;
- Data processing with the Faro Scene v. 4.1 software.

Regardless of the instrumentation and the processing method used, the process for the restitution of the acquired data was as follows (Fig. 2):

- Acquisition;
- Manual (or automatic) cleaning of the point cloud in order to eliminate any noise elements;
- Cloud processing to obtain the triangular model (or another type);
- Texturing of the polygonal model (using the frames captured by the integrated camera, obtaining a 3D representation of the artefact).
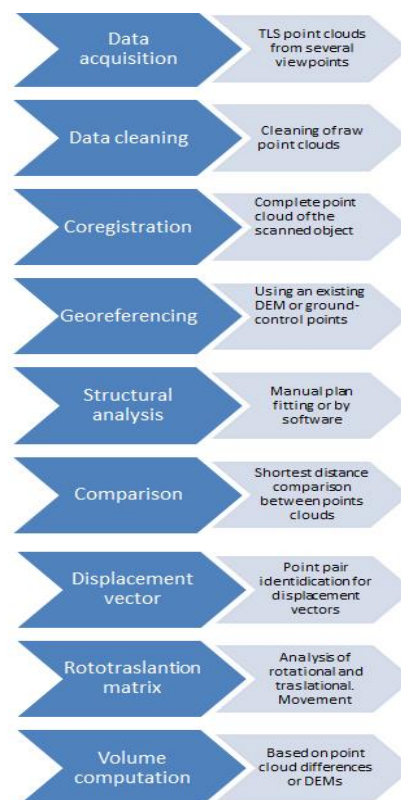


**Figure 2**: Laser scanning flow chart: Acquisition - Data processing.

However, we observed that the study area has complex geometries and requires a high level of detail for data acquisition. The survey was therefore problematic (Barrile, Meduri, & Bilotta, 2011).

In the following sections, we provide details of each procedure followed.

#### 2.1.1. Laser scanner Riegl LMS z420i

The first survey of the area was executed with the Riegl LMS-Z420i laser scanner, integrated with the Nikon D70

camera, the laser fixed, for capturing pixels for point colouring and subsequent texturing of the model.

Data acquisition in the part of the studied soil was carried out without using fixed targets, deemed unnecessary for the type of survey performed.

The research was concerned with the application of Artificial Intelligence (AI) techniques for processing and aligning images from 3D scanners, capable of generating 3D digital models. Our MATLAB algorithm was used to perform the registration of the scans, using the Iterative Closest Point (ICP) algorithm. As known, this algorithm without the help of a target carrier, allowed us to generate a single point cloud representative of the investigated object according to the flow chart presented in Figure 3.
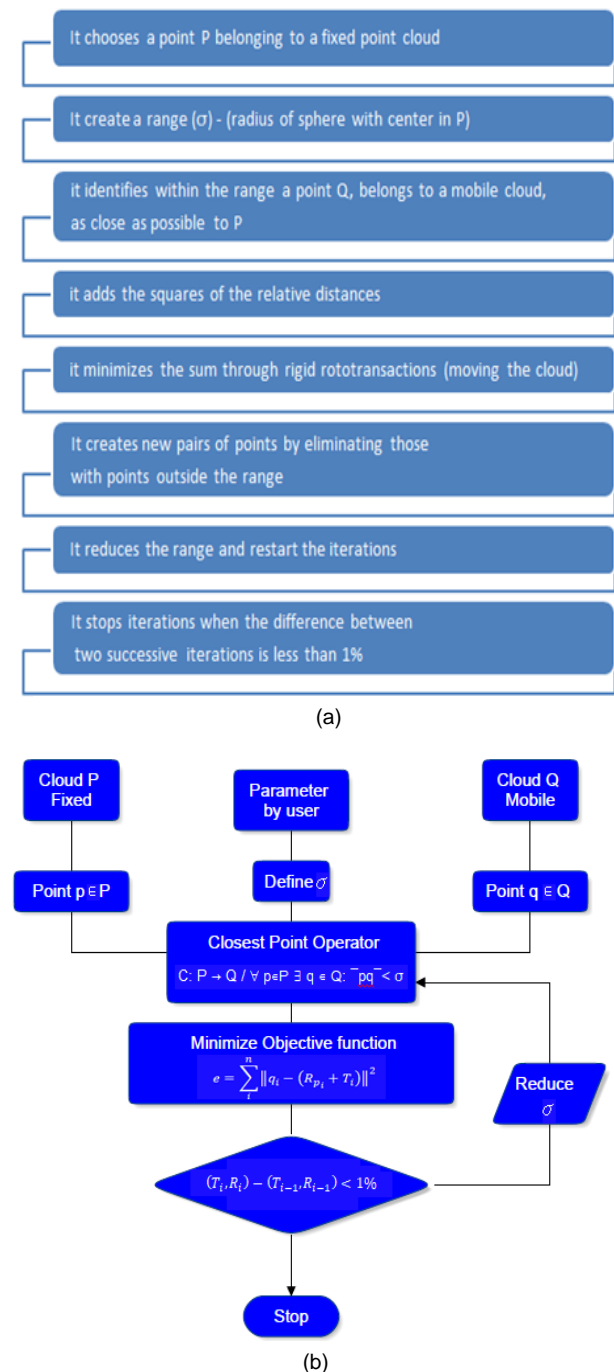


(a)



(b)

**Figure 3**: a) ICP algorithm; b) Flow chart ICP algorithm.

The tool was effective in obtaining a 3D model of the church by starting with the data gained by the scans after positioning the tool both inside and outside the building. Subsequently, the filtering operation was performed to eliminate any double points or other types of error obtained during the survey phase; the various scans were then aligned to obtain the complete 3D model of the church. (Kraus, 2007; Monti, Brumana, Achille, & Fregonese, 2004). As the errors found were between 1 and 3 mm, the 3D model obtained has high metric reliability (Akca & Gruen, 2007).

### 2.1.2. Laser scanner Faro Focus 3D

The Faro Focus3D laser scanner is a user-friendly device owing to its very simple graphical interface and easily managed by a touch screen (Fig. 4).

Scanning points were established a priori to identify any complex surfaces or shadow areas produced by the surrounding elements.

The number of stations was calculated with particular attention to ensuring an overlapping area between contiguous scans allowing the subsequent processing steps to be taken.

The survey was executed in a single day. Once the desired scan parameters had been set, the instrument was positioned in the pre-defined positions, restoring, where necessary, the orthogonality conditions by acting on the instrument tripod so that the internal electronic bubble checked the limits within which the compensator could operate to achieve perfect horizontality (Akca and Gruen, 2007).

The scans were set at a one-point resolution every 4 mm in both directions.

The survey has provided 12 measurement stations (12 scans). Having acquired the data, the next step was data processing.

Using software designed by the laser scanner manufacturer, Faro Scene v. 4.1, we processed the raw data obtained by the instrument, and then we developed the registration phase in two parts.

In the first, the entire point clouds were considered for high alignment errors following a procedure for eliminating unneeded or erratic points in the clouds (Figs. 5 and 6).

Then we repeated the procedure to verify the errors obtained. In particular, we aligned the clouds ensuring the geometric information acquired from each scan. Alignment errors identified by the software in the various attempts were between 3 and 7 mm in height. For this reason, a largely manual editing process was performed to eliminate all unsuitable points.

The collimation and registration operations were performed by recognising the characteristic points of the detected structure (edges and vertices). After repeating the registration procedure, the new alignment errors identified by the software were found to be between 1 and 3 mm. The union of the scans through the classic procedure, identifying the homologous points resulted in a cloud of points with a pitch in the lower region of about 1 mm and in the upper region around 3 mm (Barrile, Nunnari, & Ponterio, 2016).

(a)



(b)

**Figure 4**: a) Stage phase with Faro Focus3D laser scanner; b) Non-georeferenced target.



**Figure 5**: Point cloud of internal scans of the church.



**Figure 6**: Point cloud of external scans of the church.

For each scanning, the cloud of points was converted into a mesh, allowing greater intuition and interpretation. Finally, a complete 3D model was obtained by projecting the RGB images onto the mesh.

The point clouds obtained were processed using Image 5.01 and JRC Reconstructor v. 3.3.2 software, thus creating an interactive 3D model in which the user can examine and visualise the 3D models of the ruins (Figs. 7, 8 and 9) (Rinaudo, Bornaz, & Ardissone, 2007).
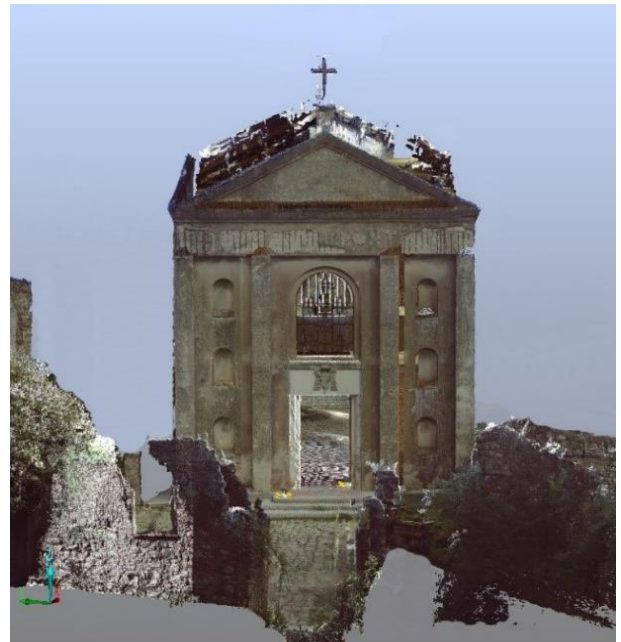


**Figure 7**: 3D model front view.



**Figure 8**: 3D model side view.



(a)                    (b)

**Figure 9**: Church altar: a) Interior 3D model, b) Zoom in.

The precision of the different methodologies of production of the 3D model (in terms of both instrumentation used and algorithms and software used

for restitution and processing) is presented in Figure 10 (Barrile & Bilotta, 2014). In particular, 12 characteristic points were identified on the two clouds (raw and clean) produced by each of the two instruments, calculating and graphing for each of them the difference (Δ raw- clean); we proceeded to calculate and plot the σ between 0 and 85 m of the difference between the two different methods with respect to the real datum.



(a)



(b)
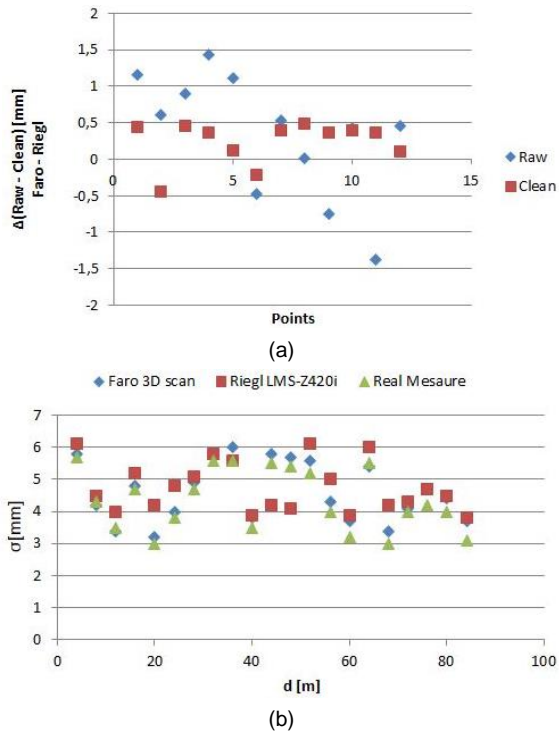
**Figure 10**: a) Comparison between difference of alignment errors (mm) of the two different methodologies in Clean and Raw Clouds; b) Comparison between errors (mm) of the two different methodologies in range position.

Figure 10a shows the delta between the errors obtained with the two instruments (Faro and Riegl, with Faro Scene v. 4.1 and Matlab algorithm, respectively) considering the Raw and Clean clouds. The graph in Figure 10b instead shows the comparison of the precision (σ) according to the acquisition distance (points to samples belonging to those elements defined with greater difficulty by the laser scans) between commercial software from Faro and Riegl and our in-house software (Matlab algorithm) with respect to the real datum.

In this regard, it should be mentioned that in relation to the verification of the metric reliability of the measurement technique, it is necessary to consider not only the precision relative to the single point as stated by the manufacturer. It is necessary to consider that the accuracy of the final data returned depends, in addition to the instrument used (acquisition precision), on the processing procedures adopted (processing precision), as processing is necessary on both the point cloud and the model.

In order to compare the processed data in a different way, it is, therefore, necessary to carry out random verification procedures of point elements, adding statistical evaluations of the deviations between 3D surfaces. In this regard, the comparisons thus made allow us to highlight that, as reported in Fig. 10a, we can

confirm that, in any case, better results were clearly obtained with clean clouds. Similarly, we can highlight a substantial difference between instruments using the commercial software and the Matlab algorithm, as clearly shown in Fig. 10b. The different tools used and the different processing methods produced similar metric results in terms of precision, further validated also by the adaptability to the real data. In summary, therefore, a substantial verification was found between the two methods used (Faro Focus 3D with commercial software processing and Riegl with Matlab processing).

## 2.2. Ground Penetrating Radar (GPR)

Due to their economic and security advantages, electromagnetic diagnostic techniques are used in a wide range of application contexts such as the diagnostics and monitoring of civil engineering structures and the detection of buried objects in the archaeological field (Conyers, & Goodman, 1997).

However, the analysis of technical-scientific literature on the subject reveals that the techniques used today for GPR data processing rely essentially on strong modelling simplifications and the use of heuristic methods are based on the experiences and knowledge acquired by the operator (Annan & Cosway, 1994).

As a result, the available information regarding the mathematical properties of electromagnetic fields is not exploited in any way (Davis & Annan, 1989; Grandjean & Gourry, 1996; Grasmueck, 1996). This may give rise to an increase in the computational load required for processing and incorrect reconstructions from which it is not possible to infer the correct position, form or the nature of objects of interest. Faced with these considerations, it becomes essential for the efficient localisation of archaeological heritage in areas of cultural artistic interest, the development of realistic electromagnetic models of the problem and fast algorithms for the processing and interpretation of the georadar data (Persico & Sato, 2017).

The results of these models, equipped with a greater accuracy level can then be exploited to support 3D modelling techniques.

The investigations were performed using the GPR IDS RIS-K2 equipment.

For the GPR campaign, we used two 200MHz and 600MHz antennas, whilst to improve radargram results we chose k parameter equal to the value of the sampling frequency of the survey campaign carried out (200 MHz); the sampling used was 100 m.

As known, in an important GPR survey, thousands of 2D images can be extrapolated requiring analysis times and necessitating expert and qualified personnel able to read single radargram. Therefore, an approach to cleaning images and reconstructions of any 3D objects would allow even inexperienced eyes, an interpretation of the data of GPR instruments.

In particular, we worked on:

### 2.2.1. Migration algorithms

Several migration algorithms were used to focus GPR rough images. It is known from the technical literature on the subject that the focusing of raw data becomes

necessary in order to locate more precisely the exact position, as well as outlining the shape of the buried objects. The techniques considered in this study were the following: Stripmap Synthetic Aperture Radar (SAR), Kirchhoff Migration (KM) and Frequency Wavenumber (FK). The techniques in question were subsequently implemented and used in focusing the GPR images collected during the measurement campaign in the reference church (Liu, Serhir, Kameni, Lambert, & Pichon, 2017).

### 2.2.2. Focusing Methods

In a rough B-scan section, obtained through a normal mono-static GPR campaign, a buried object may appear in the form of a hyperbolic trace. Wave Focusing (or migration) means a set of methods that can improve B-scan quality by mitigating the effects of the hyperbola. Thus, in the results, the processed and displayed object form is closer to its physical dimension by giving a more accurate spatial placement.

In the following paragraph, we provide a brief account of the focusing techniques used further for the measuring campaign.

2.2.2.1. - Diffraction Summation

When a mono-static GPR moves along a y-axis scan line, a buried object located at the coordinate point ($y_a$, $z_a$) results in a hyperbolic trace displayed in a B-scan.

The Diffraction Summation technique is the simplest approach for target focus tracking. It works as follows: If $\Psi$ is the representative scalar field of the data collected along the $y$ scanning line, the focal field $\Psi_f$ can be obtained as the sum of each point within the raw B-scan along the hyperbolic curve of diffraction with the velocity of the waves in the middle obtained using the "exploding source" model. If the electromagnetic properties of the ground where the object is buried varies slowly, a single velocity $v_e$ can be used for the whole extension in depth (i.e. the medium can be considered homogeneous).

2.2.2.2. - F-K migration

FK migration (or Stolt migration) can be considered as a variant of the Phase Shift method, valid only for a constant value of $v_e$. It can be shown that the expression of $\Psi_f$ can be evaluated by Fourier inverse transform, therefore it is computationally significant and in the detail it is possible to obtain the data focusing $\Psi_f(y,z)$ as simply the product's Fourier inverse transform between $kz/\omega$ and the two-dimensional Fourier transform Y for the raw data. A logical graphical representation of the method is shown in Figure 11 (Ortega-Ramirez et al., 2018).

The investigative campaign that allowed us to gather a multitude of data on which to test the proposed algorithms was conducted in the Church of Africo Vecchio (Fig. 12).

The logic scheme used for GPR scans is shown in Figure 13. In order to obtain a better data correlation during post-processing, the surveys were performed to create a network that better covered the survey surface, as seen in Figure 13; where each line represents a strip of the antenna (radargram). The data

was collected in real time on the laptop connected to the system that allowed the immediate visualisation of the single radargram. This allowed us to reduce any errors in conducting the swipe and, at the same time, highlight points or areas worthy of specific insights.

The following sequence of processing was taken before focusing: i) first time alignment, ii) dewow, iii) background removal, iv) time gain. All processing routines were implemented in the MATLAB environment and run on a PC supporting the 64-bit Intel Core 2 Duo 1.66GHz 2 MB L2 cache and 4 GB ECC fully-buffered DDR2 RAM. From the profiles collected during the survey campaign, two B-Scan (Figs.14a and 15a) are shown. On these profiles, the migration techniques mentioned above were applied: Diffraction Summation algorithm (Figs. 14b and 15b) and F-K algorithm (Fig. 16).
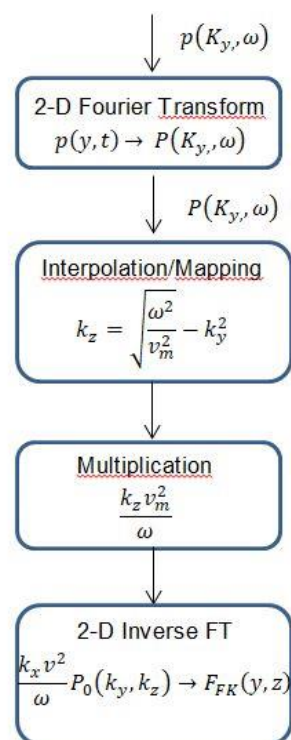


$$p(K_y, \omega)$$

2-D Fourier Transform
$$p(y,t) \rightarrow P(K_y, \omega)$$

$$P(K_y, \omega)$$

Interpolation/Mapping
$$k_z = \sqrt{\frac{\omega^2}{v_m^2} - k_y^2}$$

Multiplication
$$\frac{k_z v_m^2}{\omega}$$

2-D Inverse FT
$$\frac{k_x v^2}{\omega} P_0(k_y, k_z) \rightarrow F_{FK}(y,z)$$

**Figure 11**: Flowchart for the practical implementation of the 2D Stolt migration.



**Figure 12**: Interior flooring of the Church.

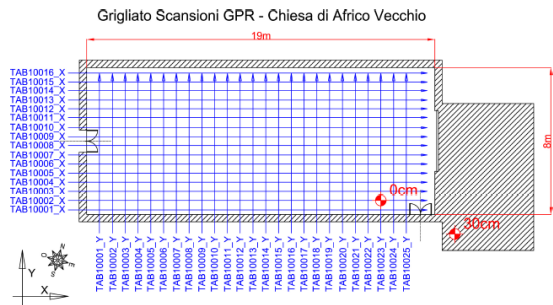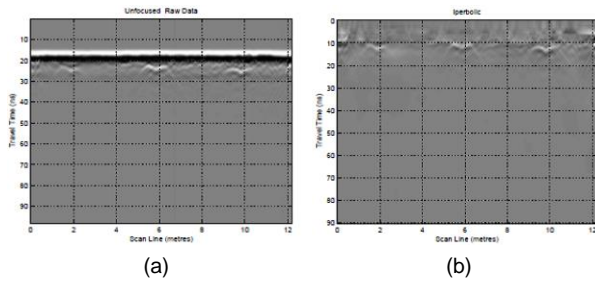**Figure 13**: Simplified plan of the Church of Africo Vecchio and its reference to the scans carried out.



| (a) | (b) |

**Figure 14**: Sample scanning 1. a): Raw B-scan; b): B-scan focused using the Diffraction Summation algorithm.
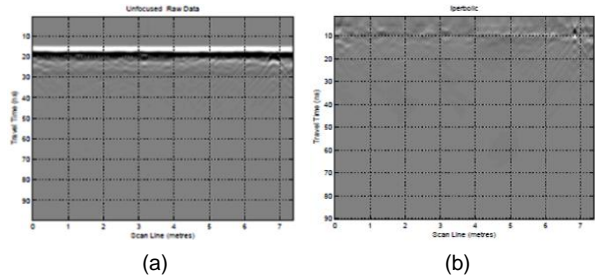


| (a) | (b) |

**Figure 15**: Sample scanning 2. a): Raw B-scan; b): B-scan focused using the Diffraction Summation algorithm.
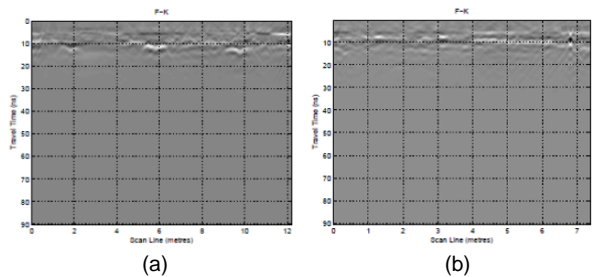


| (a) | (b) |

**Figure 16**: B-scan focused using the F-K algorithm. a) Sample scanning 1; b) Sample scanning 2.

**Table 1**: Comparison of the execution times of the focusing algorithms used in this work

| Method | GPR 1 Profile | GPR 2 Profile |
|---|---|---|
| Kirchhoff Migration | 88.71 s | 36.83 s |
| F-K migration | 2.59 s | 1.68 s |

In addition, analysis of the increase in image gains was conducted. The results showed highlight the acceptable gain limit threshold, and subsequently, the results of the assumed migration amplitude values of the interest signal so as to be confused with the background, making the radargrams unreadable and lacking in useful information. Table 1 shows the comparison of the execution times of the focusing algorithms used.

In the study area, no additional archaeological assets were identified in the first acquisition, and further investigation and improvements to the algorithm are necessary thus.

## 2.3. 3D GPR Model by Matlab

In order to carry out the 3D reconstruction of both the visible part (through the laser scanner) and subsoil part (through the GPR) of the survey area, a 3D model was reconstructed from georadar surveys.

The output radargrams of the migration process were used as input to back-scattering (BS) codes, produced in MatLab environment that allows the albeit raw reconstruction of the buried object with a different dielectric constant to subsoil.

In general, the BS codes make a change of domain from time to frequency that allowed the retrieval of the information necessary to reconstruct the 3D model, which the radargram currently does not permit.

In general, the study of the signal, or processing, on Matlab, can be developed through a series of operations, specifically:

- Reading of data by the software;
- Graphic representation of the signal;
- Signal normalisation;
- Background noise reduction;
- Application of a filtering code;
- Signal amplification;
- Graphic representation after processing.

In our case, we, therefore, created a cell-type element, which is a structure that allows the grouping of different data, thus bringing together all the scans carried out in a single variable. Each scan was saved as a matrix consisting of a pre-defined number of lines and a number of columns that vary according to the length of the scan itself.

Radar data were initially processed using standard 1D and 2D techniques.

Time band maps were constructed based on the average amplitude (or square amplitude) of the radar signal within consecutive $\delta t$ (theoretical time for the reflection of electromagnetic waves at a given depth) width time windows (Goodman, Nishimura, & Tobita, 1994).

The previous spatial average was also useful for reducing the noise of small-scale heterogeneity. Finally, the data was interpolated and cross-linked on a regular mesh.

The selection of the various parameters involved and in particular the width of the band, equal to $\delta t$, is very important. Typically, $\delta t$ must be of the order of the dominant period, but it is possible to use different widths to improve particular characteristics.

In common practice, non-overlapping time windows were chosen. In fact, the use of continuous time windows has higher computational costs, although it has the advantage of producing a higher resolution.

The traces of the radar were thus represented in continuous lines where the shape of the transmitted wave of each track stacked in a horizontal direction, composed of coordinates.

For each file, the traces that fall within a two-dimensional (2D) horizontal search window around a volume cell were transformed and stacked together.

After all the data files had been processed, the value of the final volume cell was calculated by calculating the average of all the entered values.

The representation of more traces provides the first feedback on the result, and it serves as a basis for the subsequent modelling.

The plot3 statement, however, does not allow the graph of real functions of two real variables as this graph is a surface and plot3 draws only lines. To draw surfaces, one should use the "mesh" and "surf" instructions.

To obtain the graph of the surface of the function $z=f(x,y)$ on the rectangle $[a,b]x[c,d]$ we proceeded firstly to construct the matrices of the coordinates of the nodes on which to evaluate the function $f(x,y)$ through

$>> [x,y]=meshgrid(a:stepx:b,c:stepy:d);$

{it constructs the matrix x in which each row is equal to $[a:stepx:b]$, and each column has the dimension of $[c:stepy:d]$, and the matrix y in which each column is equal to $[c:stepy:d]$ and each line has the dimension of $[a:stepx:b]$}

The matrix of the heights $z\_ij = f(x\_i,y\_j)$: is then calculated $>> z=f(x,y)$;

$>> mesh(x,y,z)$

The mesh command creates the 3D perspective plot of the $z$ values.

If we want to see the surface from another angle, we can use the function

$>> view (angle, elevation)$

where angle represents the angle between the y-axis and the point of view measured on the $x$-$y$ coordinate plane and elevation is the angle between the $x$-$y$ coordinate plane and the point of view.

Matlab also allows us to rotate the surface interactively on the current window using the mouse and the "rotate3d on" command (Sigurdsson & Overgaard, 1998).

In summary, therefore, the approach used to display 3D radar data can be summarized as follows:

1. Extraction of the most important complex signal attributes;

2. Elaborate 2D in the different directions of the areas of interest;

3. Choice of the threshold value;

4. 3D rendering of the alleged target.

Figure 17 shows the result of 3D processing, in relation to the study case, according to the previous methodology. The result shown is today the best among all those elaborated, it emphasises that the 3D reconstruction from georadar does not provide well-defined 3D edges, but only raw reconstructions of

the dimension of the buried object identified, due to the heightened variability of the dielectric constant as a humidity function.

In fact, to obtain this reconstruction, we employed the contrast of $\varepsilon_r$, the one situated in the ground that is known and the other –buried objects– that are unknown.
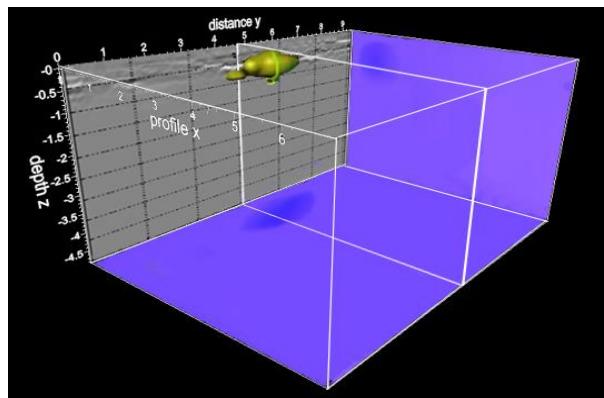


**Figure 17**: 3D rendering of buried object from GPR survey processed with in-house MATLAB algorithm.

## 2.4. Augmented reality (AR)

With a view to disseminating and enhancing cultural heritage, the Geomatica laboratory in Reggio Calabria is working on developing a tourism app in an augmented and virtual reality environment. In this regard, in this case study, the aforementioned app has been implemented in such a way as to allow the user not only to see the 3D model but also information of augmented reality. Therefore the user is able to perform a simulation scanning with the GPR, whilst in the future, enlarge the study area near the church, which returns a 3D model of objects detected by the GPR directly on the screen (Barazzetti, Remondino, & Scaioni, 2010).

AR is an effective tool to promote the process of disseminating information and enhancing cultural heritage (Bae, Golparvar-Fard, & White, 2013; Cuca, Brumana, Scaioni, & Oreni, 2011). This technology allows the addition of virtual content to a physical environment interactively and in real time. In addition to enriching virtual contents with what is real, it actually actives the connections that man perceives in the world around him. The new technology produces a virtual 3D content onto a physical environment, in an interactive and real-time format. The founding elements of any AR system are tracking, real-time rendering and visualisation technologies. Therefore, tracking is fundamental. It is a matter of recording the position of the observer, of real and fictitious objects. Precise and fast-tracking is essential for the correct visualisation of the virtual components of the scene (Brumana, Oreni, Caspani, & Previtali, 2018).

The environment for developing the app was Unity 3D. It is a multi-platform tool for creating interactive 3D content, such as architectural visualisations or 3D animations in real time, using two different programming languages, customised JavaScript based on languages. NET and C ++.

Unity's programming work is based on the use of objects: the so-called "Game Objects"; they can have or

not have a graphical representation. To them, scripts can be associated, which defines their behaviour using particular event functions. Unity is integrated by software development kit (SDK) Vuforia.

Vuforia is the most used platform in the world for the development of augmented reality. From an operational standpoint, this SDK is based on the real-time tracking of images and objects. On these targets, or "Markers", it is possible to place virtual elements (e.g. 3D models), which are then displayed on the screen according to the observer's perspective. One of the main strengths is the freedom to choose these Markers. In fact, the framework allows the recognition of words, objects and images, with even more than one at the same time, previously scanned through special tools, and made available to developers.

The app that was created is a tourist app for mobile devices that allows the user to be able to view the 3D model in AR, in real time, and to have additional information on the object observed (Fig. 18) (Barrile, Fotia, & Bilotta, 2018). The model is further refined in the phase of automatic reduction of edges and the vertices of the mesh, in order to improve and make the 3D models integrable and manageable by reducing their dimensions without losing in metric precision. Therefore, the user makes a virtual tour inside (with a viewer or simply through the screen of the device), always "accompanied" during the visit by a virtual guide that interacts with the surrounding environment (Merino, Márquez, & González, 2018).
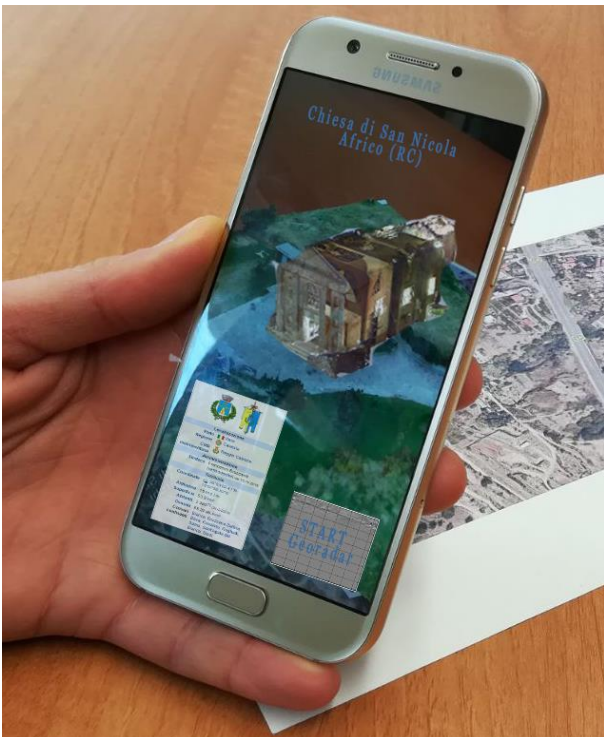


**Figure 18**: Visualization of the 3D model in AR during the framing of the map of Africo, with the possibility to access the information of the place and the start of the GPR simulation.

Portable devices support location-based technologies such as Radio-frequency identification (RFID) and near field communication (NFC), as well as other means for the geolocation of the device such as Global Navigation

Satellite System (GNSS) and QR code reader; through these functionalities, these devices allow us to receive and transmit localised and contextualised information and to satisfy users' preferences by transmitting their personalised and specific information.

The tracking process has provided with the presence of markers, seen in the example a wall of the church which is displayed with additional information or even its inside, with the correlation between the real coordinates detected through the device GPS, and the coordinates of the georeferenced 3D model.

The process of iteration of real/virtual coordinates means that, once the app is started, whenever the user is within a pre-established range of the identified area, he will be informed immediately, through notification, and be able to make a virtual tour accompanied by a virtual guide that provides information.

In the study area, following a markerless tracking process (interaction between GPS coordinates of the device and real coordinates of the study area) the developed app allows the user, among other things, to simulate the survey carried out by GPR through the device camera.

So, when the coordinates detected by the GPS of the mobile fall within a pre-established range in the construction phase of the app, it starts a simulation of the survey displaying the GPR 3D model

Although the investigations of the GPR in the study area gave a negative result (Figs. 14, 15 and 16), it was indeed minimal, characterised by a long and thin shape, in a non-deep zone (depth only 30 cm), that resulted in being a piece of old pipe.

It appears on the display when the GPS coordinates of the device are within the range of the study area, meanwhile the cameras are performing the simulation of GPR scanning, showing the resulting scan. The result obtained is shown in Fig. 19.
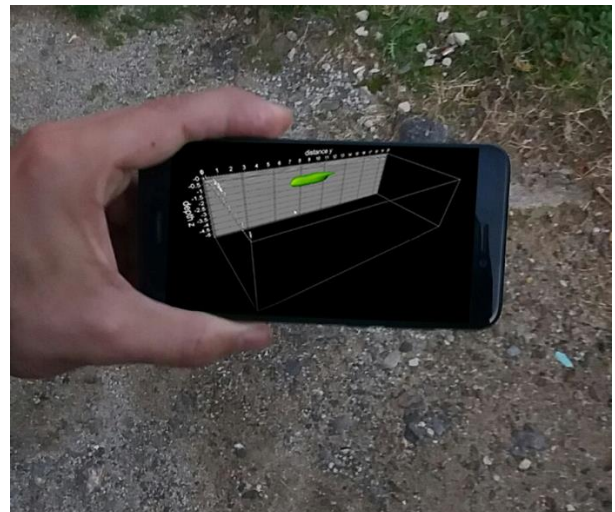


**Figure 19**: Visualization of the 3D model in VR during the GPR simulation by device camera.

The difficulty then in developing the app has been the coexistence of the environment of AR with other technologies such as GPS, the accelerometer of the phone, and data location.

Specifically, as regards to Vuforia, the configuration is limited to replacing the traditional Unity camera with a modified version: the AR Camera. At this point, after setting the desired Marker, it is sufficient to place the virtual objects that are to be shown to the user in a hierarchically inferior position with respect to the object representing the target in the scene. During the execution, Vuforia will automatically deal with the recognition of the Marker via video camera, and then the visualisation of virtual objects according to the user's perspective.

The Unity accelerometer provides a unified interface independent of the device: Input.acceleration, which consists of a Vector3 and corresponds to the gravitational acceleration of the device.

Since the axis orientation can vary from device to device, a control on the type of device used has been inserted into the code, which allows reordering of the axes.

As for the connection between the client devices and the server, we used the Multiplayer protocol made available by the game engine. This allows the definition of network objects, whose status is automatically synchronised between the various devices belonging to the same defined a priori by the programmer.

With this clarification, we can state that the classes responsible for managing this aspect are two: Buffer and Data-Provider.

The Buffer, due to the use of the Singleton pattern, has the task of maintaining a copy of the data of the objects to be displayed by the clients. This class provides the procedures for the addition, updating and removal of data, ensuring their consistency due to the control of reading and writing made by the lock on the object itself.

The Data-Provider instead deals with the actual sending of data to the client.

This Unity script, linked to a Game Object running on both the server and the client, is responsible for verifying in each frame the presence of new data inside the Buffer and therefore, based on these, to update its representation both on the server side that client side. This effect is achieved thanks to the use of the RPC functions.

Therefore, based on the content of the buffer, the action to be taken on the object under examination is chosen and executed both on the version of the object maintained on the server and on those maintained by clients.

## 3. Discussion

Through an interdisciplinary dialogue between traditional geomatic techniques and new technologies in the virtualisation sector, we can improve the documentation and provide the public with a useful tool for greater understanding, enhancement and conservation of the cultural heritage that surrounds us.

On the one hand, the high metric reliability derived from traditional tools allows the reconstruction of models which are very reliable with acceptable errors. On the other hand, the use of virtual and AR applications allow the user to see associated multimedia contents and information directly on the subject of investigation.

Specifically, in relation to this note, the in-house development of algorithms for data processing has produced some unexpected results. In fact, despite the use of two different instruments and two data processing methods, the results obtained in terms of metric (σ) are widely comparable when the range varies, while significant variations are highlighted using Clean and Row data, respectively.

Regarding the survey and the restitution from georadar, we observed, as expected, that the algorithms used for the restitution of the 3D model improved in terms of precision when the survey mesh is denser (greater number of vertical and horizontal lines), noting on the other hand that the precision decreases when increasing the depth of investigation.

Noteworthy results can be considered in what occurred in terms of interaction between GPS coordinates entered in the app implementation software and coordinates detected on site by mobile devices used to perform functional tests. In fact, the same devices (although they are known to have poor GPS accuracy) send notification of activating the app in perfect correspondence with the actual study area identified.

Moreover, in addition to the creation of various data processing algorithms, building up a specific tourist app that can be easily consulted for the management of metrically precise 3D models which, to date, would be difficult to integrate and manage, given the large size of the models themselves.

## 4. Conclusions

The final goal is the integration of three different methodologies (TLS, GPR, 3D modelling) that when combined are able to display three-dimensionally on the surface (through the laser scanner), and in the substrate (through the GPR) the survey area, in order to create an educational app. Obviously, the app created in this way is to be further improved through other enhancements in the virtual reality area, providing valuable support in the field of archaeological/cultural heritage, for the dissemination and use of information for mainly tourist purposes.

The study presented here compares the results of two different methods (instrumentation and processing methods) for 3D acquisition through laser scanner and for GPR localisation of any buried archaeological remains.

The results obtained can be integrated into WebGIS, and/or made available through Android apps, for smartphones and tablets.

In addition, virtual reality and AR can be used to integrate the real world with information of different origins enriched with graphic, textual and media information.

The aims can be both historical research, or studies related to the history of the territory, for either educational or cultural purposes. Virtual models with their realism are becoming community assets, and also raise awareness of the cultural value of the territory.

They encompass all methods for acquiring information about archaeological and architectural heritage and spreading it.

The goal of future research will also be to increase the 3D modelling and retrieval of data from GPR, as described in this research with the aim of contributing to the valorisation of archaeological heritage in areas of artistic and cultural relevance.

The above methodologies already implemented within the app, if enhanced and further refined, will allow even better dissemination of archaeological and cultural information.

## References

Akca, D., & Gruen, A. (2007). Generalized least squares multiple 3D surface matching. *ISPRS WS Laser Scanning 2007, 36*(3), 1-7. https://doi.org/10.3929/ethz-a-005748609

Annan, A. P., & Cosway, S. W. (1994). GPR frequency selection. In *Proceeding of the Fifth International Conference on Ground Penetrating Radar (GPR '94), June 12-16, Kitchener, Ontario, Canada*, 747-760.

Bae, H., Golparvar-Fard, M., & White, J. (2013). High-precision vision-based mobile augmented reality system for context-aware architectural, engineering, construction and facility management (AEC/FM) applications. *Visualization in Engineering 1*(1), 1-13. https://doi.org/10.1186/2213-7459-1-3

Ballabeni, A., Apollonio, F. I., Gaiani, M., & Remondino, F. (2015). Advances in image pre-processing to improve automated 3D reconstruction. *International Archives of the Photogrammetry, Remote Sensing and Spatial Information Sciences Archives*, *XL-5/W4*, 315-323. https://doi.org/10.5194/isprsarchives-XL-5-W4-315-2015

Barazzetti, L., Remondino, F., & Scaioni, M. (2010). Orientation and 3D modelling from markerless terrestrial images: Combining accuracy with automation. *Photogrammetric Record*, *25*(132), 356-381. https://doi.org/10.1111/j.1477-9730.2010.00599.x

Barrile, V., & Bilotta, G. (2014). Self-localization by laser scanner and GPS in automated surveys. *Computational Problems in Engineering. Lecture Notes in Electrical Engineering*, Springer, 307, 293-313.

Barrile, V., Fotia, A. & Bilotta, G. (2018). Geomatics and augmented reality experiments for the cultural heritage. *Applied Geomatics.* https://doi.org/10.1007/s12518-018-0231-5

Barrile, V., Nunnari, A., & Ponterio, R. C. (2016). Laser scanner for the Architectural and Cultural Heritage and Applications for the Dissemination of the 3D Model. *Procedia: Social & Behavioral Sciences*, *223*, 555-560. https://doi.org/10.1016/j.sbspro.2016.05.313.

Barrile, V., Meduri, G. M., & Bilotta, G. (2011). Laser scanner technology for complex surveying structures. *WSEAS Transactions on Signal Processing*, *7*, 65-74.

Brumana, R., Oreni, D., Caspani, S., & Previtali, M. (2018). Virtual museums and built environment: narratives and immersive experience via multi-temporal geodata hub. *Virtual Archaeology Review*, *19*(9), 34-49,. https://doi.org/10.4995/var.2018.9918.

Conyers, L. B., & Goodman, D. (1997). *Ground-Penetrating Radar - An Introduction for Archaeologists*. Walnut Creek, CA: AltaMira Press, A Division of Sage Publications*, Inc.*

Cuca, B., Brumana, R., Scaioni, M., & Oreni, D. (2011). Spatial data management of temporal map series for cultural and environmental heritage. *International Journal of Spatial Data Infrastructures Research, 6*, 1-31. https://doi.org/10.2902/1725-0463.2011.06.art5

Davis, J. L., & Annan, A. P. (1989). Ground-penetrating radar for high-resolution mapping of soil and rock stratigraphy, *Geophysical Prospecting, 37*, 531-551. https://doi.org/10.1111/j.1365-2478.1989.tb02221.x

Kraus, K. (2007). *Photogrammetry–Geometry from images and laser scans.* Berlin: Walter de Gruyter.

Goodman, D., Nishimura, Y., & Tobita, K. (1994). GPRSIM forward modeling software and time slices in ground penetrating radar surveys. In *Proceedings of the Fifth International Conference on Ground Penetrating Radar (GPR '94), June 12-16, Kitchener, Ontario, Canada,* 31-43.

Grandjean, G., & Gourry, J. C. (1996): GPR data processing for 3D fracture mapping in a marble quarry (Thassos, Greece). *Journal of Applied Geophysics*, *36*, 19-30. https://doi.org/10.1016/S0926-9851(96)00029-8

Grasmueck, M. (1996): 3D ground-penetrating radar applied to fracture imaging in gneiss. *Geophysics*, *61* (4), 1050-1064.

Liu, X., Serhir, M., Kameni, A., Lambert, M., & Pichon, L. (2017). Ground penetrating radar data imaging via Kirchhoff migration method. In *Applied Computational Electromagnetics Society (ACES 2017)*, Mar 2017, Florence, Italy,1-2. https://doi.org/10.23919/ROPACES.2017.7916395

Merino, A., Márquez, C., & González, R. (2018). APP 3D: sculpture cycle of the Torreparedones forum (Baena, Córdoba). *Virtual Archaeology Review*, *19*(9), 89-101. https://doi.org/10.4995/var.2018.9424

Monti, C., Brumana, R., Achille, C., & Fregonese, L. (2004). *Per un moderno rilievo della basilica di San Lorenzo tra opera, progetto e trasformazioni.* Milan: Silvana Ed.

Ortega-Ramirez, J., Bano, M., Villa-Alvarado, L. A., Junco-Sanchez, R., Pifia-Cetina, M., Estrada-Apatiza, S., Vera-Sanchez, J. C., & Hernández-López, A. (2018). Ground penetrating radar investigation of an ancient Spanish fortress: The Fort of San Diego, Acapulco, Mexico. In: *17th International Conference on Ground Penetrating Radar (GPR)* 18-21 June 2018, 1-4. https://doi.org/10.1109/ICGPR.2018.8441550

Persico, R., & Sato, M. (2017). Ground-Penetrating Radar: Technologies and Data Processing Issues for Applications in the Field of Cultural Heritage. In: N. Masini, & F. Soldovieri (Eds), *Sensing the Past. Geotechnologies and the Environment (pp. 175-202),* Cham: Springer. https://doi.org/10.1007/978-3-319-50518-3_9

Rinaudo, F., Bornaz, L., & Ardissone, P. (2007). 3D high accuracy survey and modelling for Cultural Heritage Documentation and Restoration. *Vast 2007–future technologies to empower heritage professionals*, November 26–29, 2007, Brighton, UK, *Archaeolingua Hun*, 19-23.

Sigurdsson, T., & Overgaard, T. (1998). Application of GPR for 3D visualization of geological and structural variation in a limestone formation. *Journal of Applied Geophysics*, *40*, 29-36.